ORIGINAL RESEARCH

Exosomal MEF2C's Association With the Progression of CRC in Regulating CD36 Transcription

Meng Wang, MD; Yujuan Jiang, MSc; Zhi-Lu Fan, MSc; Na Zhang, MSc; Jianwei Liang, MD; Zhaoxu Zheng, MD

ABSTRACT

Context • Exosomes are biologically active, extracellular vesicles that are involved in tumor-related processes, including activating tumors, facilitating tumor growth, and promoting inflammation.

Objective • The study intended to investigate microRNAs (miRNAs) in exosomes that are associated with colorectal cancer (CRC).

Design • The research team performed bioinformatics analysis, extracting RNA-sequencing (RNA-seq) datasets from the Cancer Genome Atlas (TCGA); ExoRBase, a database of different types of RNA information that scientists have extracted from human exosomes; and the Gene Expression Omnibus (GEO) databases, and analyzed the data.

Setting • The study took place at the Department of Colorectal Surgery at the Chinese Academy of Medical Sciences and Peking Union Medical College in Beijing, China.

Participants • From October 2020 to March 2021, a total of 28 CRC patients who underwent curative resection at the National Cancer Center were enrolled. Tumor samples and tumor-adjacent normal sample were obtained from these CRC patients. Postoperative pathological characteristics all shown adenocarcinoma. The research team recruited participants from the hospitals connected with CAMS and PUMC and obtained written informed consent from them for publication of a case report and any accompanying images. The Ethics Committee of the Cancer Institute (Hospital), CAMS & PUMC has officially recognized the study (NCC 2017-YZ-026).

Outcome Measures • The research team: (1) extracted RNA-seq datasets from the TCGA, exoRBase and GEO and analyzed the differentially expressed genes (DEGs); (2) performed a cluster analysis of variant genes using weighted gene co-expression network analysis (WGCNA); (3) verified expression of myocyte enhancer factor 2C–genecards (MEF2C) and cluster of differentiation 36 (CD36) in CRC tissues; (4) explored the biological function of the MEF2C by performing proliferation, migration, and invasion assays; and (5) used a chromatin immunoprecipitation (ChIP) experiment to analyze mechanisms to reveal CD36 transcription regulated by exosomal MEF2C.

Results • A significant mean difference in exosomal MEF2C existed between normal and tumor tissues. By performing a correlation analysis, the research team found 609 potential target points of exosomal MEF2C ($r > 0.5$, $P < .05$). Weighted correlation network analysis (WGCNA) and protein-protein interaction (PPI) network analysis indicated that CD36 may be the target of exosomal MEF2C. Univariate, multivariate, and Kaplan-Meier analyses showed that CD36 was closely related to the overall survival (OS) of CRC patients. Obvious differences existed in the expression levels of MEF2C and CD36 in CRC and normal tissues according to qPCR and immunohistochemical assays. Functional-experiments analysis in vitro showed that exosomal-MEF2C could be considered as an antioncogene. Mechanistically, ChIP assays showed that MEF2C regulated the transcriptional level of CD 36; thus, the expression of CD36 increased significantly.

Conclusion • MEF2C is a potential biomarker of a favorable prognosis in CRC and is related to the progression of CRC. Moreover, the MEF2C-CD36 pathway may reveal the tumor regulation mechanism in CRC. The exosomal MEF2C was the hub gene in exosomes, with CD36 was identified as the potential target. Exosomal MEF2C may be a promising molecular biomarker for predicting a good prognosis and may have potential as a medical target for CRC. (*Altern Ther Health Med.* 2023;29(1):198-209).

Meng Wang, MD, Doctor; Yujuan Jiang, Master; Jianwei Liang, MD, Professor; and **Zhaoxu Zheng, MD,** Professor; Department of Colorectal Surgery; National Cancer Center, National Clinical Research Center for Cancer, and Cancer Hospital; Chinese Academy of Medical Sciences and Peking Union Medical College, Beijing, China. **Zhi-Lu Fan, Master**, and **Na Zhang, Master**, Wang Mingrong State Key Laboratory, National Cancer Center/National Clinical Research Center for Cancer/Cancer Hospital, Chinese Academy of Medical Sciences and Peking Union Medical College, Beijing, China.

Corresponding author: Zhaoxu Zheng, MD
E-mail: zzx_20003@126.com
Corresponding author: Jianwei Liang, MD
E-mail: liangjw1976@163.com

Worldwide, colorectal cancer (CRC) ranks second among cancer-related causes of death.[1] Despite significant improvements in treatment and diagnosis, CRC still results in approximately nine-million deaths each year.[2] Medical practitioners can treat CRC patients with laparoscopic surgery or resection, combined with either neoadjuvant or adjuvant chemotherapy.[3] However, such treatments aren't possible for the majority of advanced CRC patients, who receive a diagnosis in a late stage.[4]

Therefore, a demand exists for investigations into the pathogenesis of CRC to find novel diagnostic and prognostic biomarkers for it that can be helpful in reducing patients' mortality. Currently, researchers consider molecular therapeutics to be promising for cancer therapy.[5] With the development of molecular biology, therapeutic strategies for CRC have become more comprehensive.

Exosomes

Recently, Linnekamp et al used diverse molecular biomarkers, such as exosomal RNA, for the selection of prognostic markers or therapeutic targets of CRC.[6] Exosomes have become the focus of cancer research because of their role in intracellular communication. They are endocytic-derived, nanoscale vesicles that cells in culture secrete and that contain microRNA (miRNA), DNA, proteins, and lipids.[7]

Exosomes can act as critical messengers between cancer cells and stromal cells by transferring content that is related to genetic information in the tumor microenvironment (TME).[8] Kim et al and Camussi et al found that exosomes can transmit oncogenes or tumor-suppressor genes to tumor tissues, regulating gene expression and inhibiting tumor development.[9,10]

Chen et al suggested that exosome transport of miR-93-5p in cancer-associated fibroblasts (CAFs) may be a potential CRC target due to its stimulating effects on CRC progression, colony formation, and inhibition of apoptosis.[11] Yin et al reported that exosomes can protect nicotinamide nucleotide transhydrogenase (NNT) - antisense RNA 1 (AS1), which is a potential prognostic indicator in CRC.[12] Taken together, increased knowledge of the functions of exosomes in CRC progression indicates that exosomes affect CRC processes, including cell proliferation, cell differentiation, immune defense mechanisms, and inflammatory responses.

Genetic Databases

With the rapid development and ubiquitous application of microarrays in biomedical research, many databases have become available. The Cancer Genome Atlas (TCGA) mainly provides basic information, including single-nucleotide polymorphisms (SNPs), RNA-sequencing (RNA-seq), miRNA-seq, and other information for approximately 633 cases of CRC.

The Gene Expression Omnibus (GEO) database is a fully available, high-throughput, molecularly abundant database with information on 3628 CRC-related genes.[13] By analyzing data from the GEO and TCGA databases, Li et al found that protein arginine methyltransferase 5 (PRMT5) was a prognostic predictor of CRC in patients and a promoter of CRC malignancy by interacting with mini-chromosome maintenance 7 (MCM7) proteins.[14]

According to the TCGA and GEO data, the "zinc finger, myeloid, nervy, and DEAF-1 (MYND)-type-containing 8" ZMYND8 gene may become a biomarker that doctors can use to predict CRC patients' prognoses. Chen et al's findings suggest that ZMYND8 expression can be an effective tool in identifying CRC risk.[15]

Using systematic analysis of RNA-seq data from the TCGA and GEO databases, Zhidong et al found a correlation between "long intergenic non-protein coding RNA 2595 (LINC02595), B-cell lymphoma 2-like protein 1" (BCL2L1), and miR-203B-3p in modulation of CRC progression.[16]

The ExoRBase was created as a database of different types of RNA information that scientists have extracted from human exosomes.[17] It contains RNA-expression profiles of various diseases based on RNA-seq data.[17] The database includes data from studies in published literature that have verified the information with experimental validation.

MEF2C

Exosomes contain transcription factors (TFs) that participate in basic, cancer-related processes, such as reducing apoptosis, promoting cancer-cell proliferation, inducing angiogenesis, facilitating replication immortality, and promoting genomic instability and mutations. Some of their most notable functions include activating tumors, facilitating tumor growth, and promoting inflammation.

TFs are vital regulators of biological processes, regulating gene expression by combining regulatory elements in promoter and enhancer DNA.[18] The disorder of transcription factors can lead to the various diseases.[19] Potthoff and Olson[20] and Latchman[21] have demonstrated that "myocyte enhancer factor 2C–genecards" (MEF2C) is a transcriptional regulator that has a key impact in controlling the process of gene expression.

MEF2C is a founding molecule of the MADS transcriptional-regulator family. An increasing number of studies have suggested that MEF2C can affect the pathways of some malignant tumors. Immune cells have a role in the tumor microenvironment (TME), which influences the progression of cancer.[22] Thus, it's possible to hypothesize that MEF2C is associated with immune infiltration.

Some studies found that infiltration of NK cells indicated a better prognosis in CRC.[23-25] NK cells can produce interferon gamma (IFN-γ) in CRC, regulating cell growth.[26] Low expression of "B-cell receptor-associated protein 31" (BAP31) can have an unfavorable effect on the prognosis of CRC.[27]

Zhang et al suggested that MEF2C could facilitate the transcription of mitogen-inducible gene 6 (MIG6) to promote resistance to gefitinib, a medication used to treat hepatic cancer cells from non-small cell lung cancer.[28] Luo et al also found that an increase in MEF3C - antisense RNA

1 (AS1) was a biomarker in gastric cancer.[29] Bishop et al found MEF2C-SS18 fusions in salivary adenocarcinoma.[30] Moreover, three studies have illustrated the functions and mechanisms of MEF2C in leukemia.[31-33] These findings indicate that MEF2C has implications for various cancers.

CD36

James Drury et al found that cluster of differentiation 36 (CD36) was associated with CRC progression.[34] CD36, a transmembrane glycoprotein (GP) receptor of approximately 88 kDa, is expressed on various cell types.[35, 36] CD36 is an antiangiogenic receptor that Chen et al found to be related to a variety of tumor tissues.[37] Zhang et al and Tsuchida et al found that a high expression level of CD36 could suppress cell progression in CRC.[38, 39] Zhang et al also found that upregulation of CD36 could modulate the apoptosis of CRC cells.[38] Love et al found that CRC cells expressed CD36, which can contribute to a better prognosis in CRC.[40] Thus, CD36 could provide potential therapeutic strategies for CRC.[41]

The current study intended to investigate microRNAs (miRNAs) in exosomes that are associated with colorectal cancer (CRC).

METHODS

Participants

From October 2020 to March 2021, a total of 28 CRC patients who underwent curative resection at the National Cancer Center were enrolled. Tumor samples and tumor-adjacent normal sample were obtained from these CRC patients. Postoperative pathological characteristics all shown adenocarcinoma. The research team recruited participants from the hospitals connected with CAMS and PUMC and obtained written informed consent from them for publication of a case report and any accompanying images. The Ethics Committee of the Cancer Institute (Hospital), CAMS & PUMC has officially recognized the study (NCC 2017-YZ-026).

Procedures

The study took place in the Department of Colorectal Surgery at the Chinese Academy of Medical Sciences (CAMS) and Peking Union Medical College (PUMC) in Beijing, China. The research team performed bioinformatics analysis, which intended: (1) to analyze the key genes in the TCGA, GEO, and exoRBase databases to determine if exosomal MEF2C was associated with CRC progression, (2) to investigate the downstream target genes of exosomal MEF2C, and (3) to verify the differences in the exosomal MEF2C and CD36 in CRC and normal tissues.

Sources. The research team: (1) extracted RNA-seq datasets from the TCGA, ExoRBase, and the GEO databases and analyzed the data, (2) retrieved the expression data of 375 tumor specimens and 32 normal specimens as well as the clinical follow-up information about CRC using the National Cancer Institute's (NCI's) Genomic Data Commons (GDC) website, (https://gdc.cancer.gov/)[42] and (3) downloaded the gene expression profiles of two primary human cancer datasets—GSE32323 and GSE110224, obtaining 17 paired samples of each, from the GEO database. Exosome data for the 32 normal samples and 12 CRC samples were available from exoRBase.

Differentially expressed genes (DEGs) and immune infiltration analysis. The research team: (1) identified and adjusted DEGs for the normal and CRC groups, considering DEGs with p values <.05 to be statistically significant DEGs; and (2) assessed immune infiltration in CRC tissues using Single-sample Gene Set Enrichment Analysis (ssGSEA) and the Genetics Society of America's (GSA's) software packages.[43]

Gene-set enrichment analysis. The research team: (1) estimated the relationship between MEF2C and CD36 using the Pearson correlation test, considering a $P < .05$ to be statistically significant; and (2) used the clusterProfiler software package (The University of Auckland, Auckland, New Zealand) to study the biological effects of selected modules using gene ontology (GO) and the Kyoto Encyclopedia of Genes and Genomes (KEGG)[44] analyses.[45]

Module determination. The research team: (1) identified the association modules using weighted gene co-expression network analysis (WGCNA), based on the Pearson correlation coefficients, and (2) described the means and standard deviations (SDs) as the average gene set (GS) and used it to screen the necessary modules.

Specimen collection. The research team fast-froze the surgically resected colorectal tumor tissue and normal tissue in liquid nitrogen and kept it in an ultra-low-temperature refrigerator for RNA extraction.

Total RNA extraction and real-time quantitative reverse transcription - polymerase chain reaction qRT-PCR. The research team: (1) isolated the RNA using an RNA Isolation Kit V2 (Vazyme, Beijing, China); (2) implemented fluorescent qRT-PCR analysis using the SYBR qPCR Mix (Vazyme) and Applied Biosystems' (ABI's) QuantStudio 5 (Beijing, China); and (3) normalized the relative mRNA expression of the tested genes using an internal control, human glyceraldehyde-3-phosphate dehydrogenase (GAPDH). The details of the primer in this experiment are: MEF2C F 5'-TCCACCAGGCAGCAAGAATACG-3', MEF2C R 5'-GGAGTTGCTACGGAAACCACTG-3', CD36 F 5'-CAGGTCAACCTATTGGTCAAGCC-3', CD36 R 5'-GCCTTCTCATCACCAATGGTCC-3'.

Immunohistochemistry (IHC) staining analysis. The research team implemented IHC as Li et al[7] has described, using an IHC SP kit (No. SP-9000, ZSGB-BIO, Beijing, China) and anti-MEF2C (1:200) and anti-CD36 (1:200) from Abcam (No. ab197070; ab133625, Beijing, China). The amplification of the IHC photographs was 20×.

Western blot experiment. The research team: (1) electrophoresed proteins from whole cells under reducing conditions on a 10% polyacrylamide gels, performing it at 180 V for one h in 3-(N-morpholino) propanesulfonic acid (MOPS) running buffer (Solarbio, Beijing, China); (2) after treatment with a blocking solution containing 5% skim milk

powder, placed the protein-free nitrocellulose membrane in a 4°C refrigerator for 12-24 hours with an antibody (1:1000 dilution); and (3) analyzed the results using Image J (National Institutes of Health, Bethesda, USA). The antibodies used were anti-Calnexin (ab133615), anti-TSG101 (ab83), anti-CD63 (ab134045) antibody, and anti-MEF2C (ab191428) antibody, all from Abcam (Cambridge, UK).

Cell culture and transfection. The research team: (1) purchased the SW620 cell line from the Cell Resource Center at the Institute of Basic Medical Sciences (IBMS), at CAMS/PUMC, (2) cultured it in F12K containing 10% fetal bovine serum (FBS) (Gibco, Beijing, China) in an incubator (Thermo, Beijing, China) with the humidity specified at 37°C and 5% CO2; and (3) used the Lipofectamine 3000 reagent (No. L3000015, Invitrogen, Beijing, China) for transfection, following the manufacturer's instructions. The pEZ-M03 vector (GeneCopoeia, Guangzhou, China) used the human MEF2C coding sequences.

Colony formation assay. For the colony-forming assays, the research team: (1) inoculated the SW620 cells (1000 cells per well) in six-well plates, (2) cultured the cells for 7 days, and (3) counted the clusters containing ≥30 cells as individual colonies.

Cell migration and invasion. For migration, the research team: (1) filled the lower chamber of a Transwell plate (Corning, Beijing, China) with 800 µl of DMEM with 20% serum (Corning, Beijing, China); (2) dripped 200 µl of 2 x 105 cells of serum-free DMEM into the upper chamber; (3) after culturing the solution for 24 hours, drew out the Transwell chamber, fixed it with a 4% paraformaldehyde fixative solution for 10 min, and then dyed it for 10 min; and (4) analyzed the relative densities of cells using ImageJ (National Institutes of Health, Bethesda, USA). For the invasion assay, the workflow remained the same as for the migration. Furthermore, the team pre-coated the Transwell membrane with Matrigel (BD Biosciences, Beijing, China).

Chromatin immunoprecipitation (ChIP) assay. The research team: (1) performed the ChIP assay using an assay kit (Abcam, Shanghai, China) according to the manufacturer's instructions (Abcam); (2) treated and fixed the SW620 cells and placed them with glycine at 37°C for 10 minutes; (3) Following the cell lysis, sonicated the genome to fragments of 200-600 bp; and (4) immunoprecipitated the lysates using as the negative control, rabbit non-immune, immunoglobulin G (IgG)-conjugated, magnetic protein A/G beads (Abcam, Shanghai, China) or anti-MEF2C antibody (Abcam). The team used PCR to analyze the precipitated solution.

Outcome measures. The research team: (1) analyzed the key genes in the TCGA, GEO, and ExoRBase databases to determine if exosomal MEF2C was associated with CRC progression, (2) used WGCNA and PPI network analysis to investigate the downstream target genes of exosomal MEF2C, and (3) used qPCR and IHC assays to verify the differences in the exosomal MEF2C and CD36 in CRC and normal tissues. Exosomal MEF2C may be a possible biological target for CRC patients.

Outcome Measures

DEGs in the TCGA and GEO databases. The research team used WebGestalt R software, v0.4.2 (The University of Auckland, Auckland, New Zealand) for the analyses. The team: (1) analyzed the differential gene expressions (DEGs) in the TCGA-CRC datasets for the tumor and normal specimens; (2) filtered those DEGs according to the threshold of the false discovery rate (FDR) <0.05 and a log2 fold change (FC) >1; (3) constructed a heatmap and a volcano plot to reveal the number of distinct genes in TCGA-CRC dataset; and (4) compared the DEGs in the normal and CRC groups in the GEO database, the GSE32323 and GSE110224 datasets.

WGCNA and key module identification. The research team specifically performed analyses on tumor tissues using the "Weighted correlation network analysis" WGCNA. The team: (1) established a gene co-expression network after combining the screened genes with the DEGs extracted from the TCGA-CRC; (2) based on TOM,[46] a web-based resource for the efficient extraction of candidate genes for hereditary diseases, used the average-linkage clustering method to cluster genes and set a minimum number of genes in each module, according to the standard of the hybrid dynamic clipped tree; (3) performed cluster analysis on the modules and merged the modules that were close together into new modules—set height = 0.25, DeepSplit = 3, and minModuleSize = 100; (4) analyzed the DEGS in the GEO datasets; and (5) next analyzed the DEGs extracted from ExoRBase datasets that the team found to be related to CRC progression.

Target genes of MEF2C in CRC. Using Pearson correlation analysis, the research team: (1) found target genes that were associated with MEF2C; (2) after combining the screened genes with the DEGs extracted from the two regions, including one from 8551 target genes and another from the online version of the database (hTFtarget: http://bioinfo.life.hust.edu.cn/hTFtarget#!/), established a gene co-expression network and determined the optimal soft threshold for the adjacency computation; (3) performed the GO and KEGG enrichment analyses using WebGestalt R, to further assess the biological functions of ME turquoise; (4) used STRING (ELIXIR, Hinxton, Cambridgeshire, UK), a database of known and predicted protein-protein interactions and Cytoscape software (University of California, San Diego, California USA) to make the protein-protein interaction (PPI) network; (5) based on data from the TCGA, analyzed the 20 hub genes and evaluated the relationship between CD36 mRNA levels and overall survival (OS) in CRC; (6) analyzed the hub genes and then used the JASPAR website, (http://jaspar.genereg.net/)[47] an open-access database used for TFs across multiple species in six taxonomic groups for an analysis; (6) performed a univariate analysis on the effects of CD36 expression on OS; and (7) conducted a gene-set enrichment analysis (GSEA) to find signaling pathways correlated with CD36.

MEF2C and CD36 in CRC. the research team: (1) next investigated MEF2C and CD36 in CRC samples using IHC and qPCR assays to further verify the co-expression

relationships; (2) also performed particle size experiments, a Western blot assay, and electron microscopy using equipment from Tanon (Shanghai, China) to extract exosomes secreted by SW620; and (3) tested the exosome release of SW620 and SW480 to detect any expression of MEF2C in CRC cells exosomes.

Function and mechanism analysis of MEF2C in CRC. Previous studies have shown that MEF2C is a very important transcription factor.[48] The research team: (1) investigated the role of MEF2C in the proliferation of SW620 cells using a colony formation assay; (2) used Transwell assays to detect the cell-migration and invasion capacity to assess the influence of MEF2C on cell migration and invasion; and (3) performed a ChIP assay in SW620 cells to examine whether MEF2C modulates CD36 transcription.

Statistical Analysis

The research team used the Student's t-test for comparing values between the control and intervention groups. $P < .05$ indicated statistical significance. The qPCR and IHC analyses were performed using GraphPad Prism v. 8.01 (univ, Beijing, China).

RESULTS

DEGs in the TCGA and GEO databases

The research team filtered 3481 DEGs. Figures 1A and 1B A show the heatmap and volcano plot, respectively, that indicate the number of distinct genes in the TCGA-CRC dataset. The team extracted 5466 DEGs from the GEO for analysis. Figures 1C and 1D show the heatmap and volcano plot, respectively, that indicate the number of distinct genes in the GEO dataset.

WGCNA and Key Module Identification

The gene co-expression network included 3481 DEGs extracted from the TCGA-CRC and the research team found that 5 was the optimal soft threshold for the adjacency computation. Figures 2A and 2B team

Figure 1. Heatmaps and Volcano Maps of DEGs. Figure 1A shows the heatmaps of DEGs in TCGA. The blue bar represents normal tissue type and pink represents tumors; Figure 1B shows the volcano map that depicts DEGs in TCGA, with the red dots highlighting the upregulated DEGs, and the green dots reflecting downregulated DEGs; Figure 1C shows the heatmaps of DEGs in the GEO database; and Figure 1D shows the volcano maps that depict DEGs in that database.

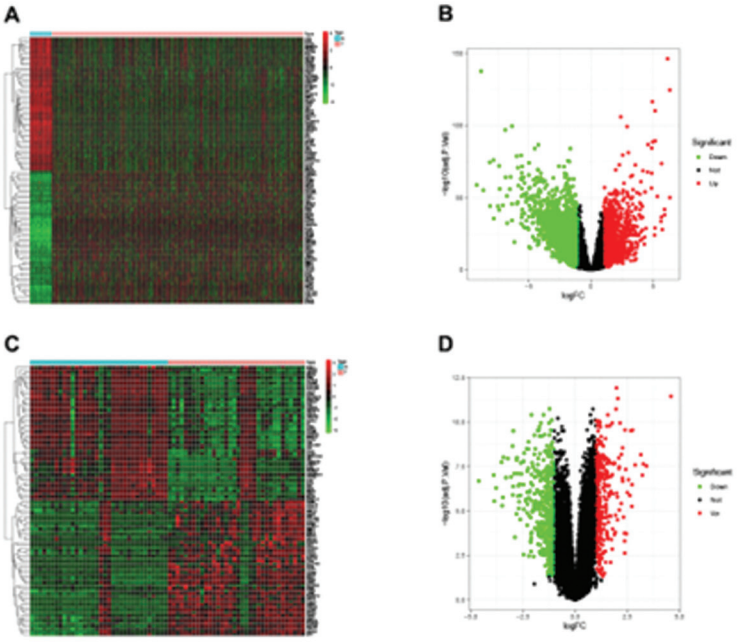

Abbreviations: DEGs, differentially expressed genes; GEO, Gene Expression Omnibus database; TCGA, Cancer Genome Atlas database

Figure 2. WGCNA of TCGA Database. Figures 2A and 2B show that the soft threshold power value was $\beta = 7$ (R2 = 0.9); Figure 2C shows the clustering dendrogram of DEGs from TCGA; Figure 2D shows that the MEyellow module was significantly negatively associated with CRC tumors; and Figures 2E and 2F show that the heat maps based on adjacencies gave similar results, illustrating the relationship between the yellow module and normal and tumor tissues, respectively.

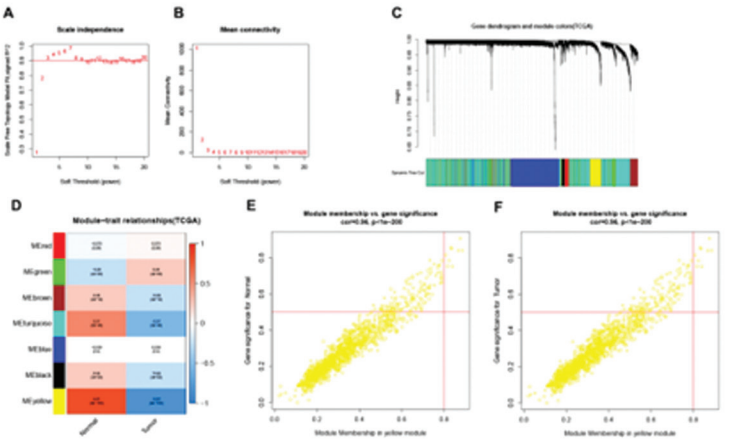

Abbreviations: CRC, colorectal cancer; DEGs, differentially expressed genes; TCGA, Cancer Genome Atlas database; WGCNA, weighted correlation network analysis

Figure 3. WGCNA Analysis of GEO Database. Figures 3A and 3B show that the soft-threshold power value was β = 4 (R2 = 0.9); Figure 3C shows the clustering dendrogram of DEGs from the database; Figure 3D shows that the MEbrown module was significantly, negatively correlated with CRC tumors, according to dynamic tree cutting analysis; and Figures 3E and 3F show that the heat maps based on adjacencies also gave similar results, illustrating the relationship between the MEbrown module and normal and tumor tissues, respectively.

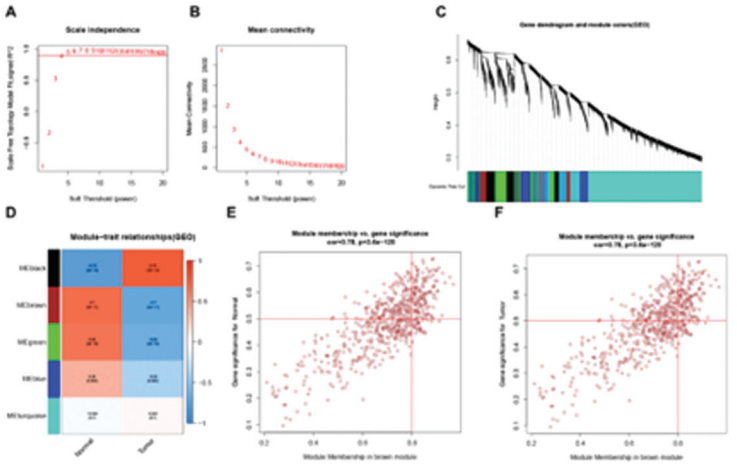

Abbreviations: CRC, colorectal cancer; DEGs, differentially expressed genes; ExoRBase, a database of different types of RNA information that scientists have extracted from human exosomes; GEO, Gene Expression Omnibus database; MEF2C, myocyte enhancer factor 2C – genecards; TCGA, Cancer Genome Atlas database; WGCNA, weighted correlation network analysis

Figure 4. Heatmaps and Volcano Maps of DEGs. Figure 4A shows the heatmaps of DEGs in ExoRBase; Figure 4B shows in a Venn diagram the intersection of 3 regions, including DEGs in TCGA-yellow, GEO-brown, and ExoRBase, indicating that the analysis found only co-differentially-expressed MEF2C mRNA; and based on the TCGA database, the expression of MEF2C was significantly lower in CRC tissues (Figures 4C and 4D) than in normal tissues (Figure 4 E).

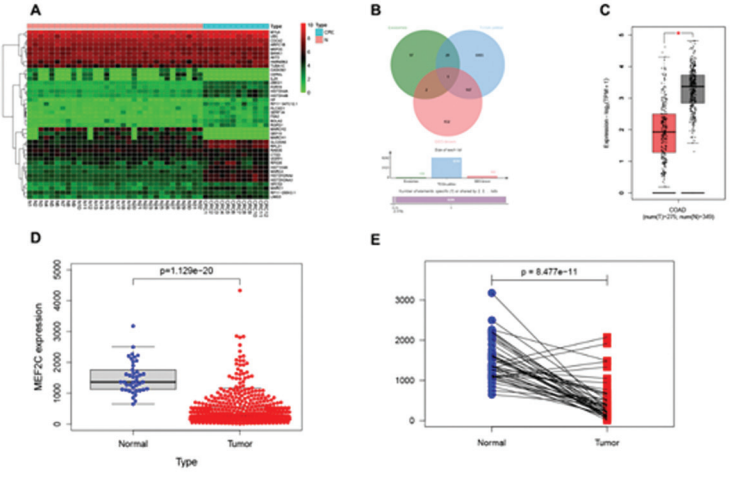

Abbreviations: COAD, Colon adenocarcinoma ; CRC, colorectal cancer; DEGs, differentially expressed genes; ExoRBase, a database of different types of RNA information that scientists have extracted from human exosomes; GEO, Gene Expression Omnibus database; MEF2C, myocyte enhancer factor 2C–genecards; TCGA, Cancer Genome Atlas database

show that the soft threshold power value was β = 7 (R2 = 0.9). The team set 100 as the minimum number of genes in each module. In the cluster analysis, the grey module represented a gene set that couldn't be aggregated into other modules.

Figure 2C shows the seven distinct modules, including red, grey, brown, turquoise, blue, black, and yellow modules, that the analysis detected in the RNA co-expression network through the dynamic tree cutting approach. As Figure 2D shows, the MEyellow module was significantly negatively associated with CRC tumors (t = 0.87, P = .000). The heatmaps based on adjacencies showed similar results, with Figure 2E illustrating the relationship between the yellow module and normal tissues and Figure 2F the relationship between the yellow module and tumor tissues.

For the 5466 DEGS in the GEO datasets, 5 was the optimal soft threshold for the adjacency computation. Figures 3A and 3B show that the soft-threshold power value was β = 4 (R2 = 0.9). The analysis of WGCNA detected five distinct modules in the GEO datasets, and the MEbrown module was significantly negatively correlated with CRC tumors (t = 0.7, P = .000), according to the dynamic tree cutting analysis (Figure 3C and D). Heatmaps based on adjacencies also showed similar results. Figure 3E illustrates the relationship between the MEbrown module and normal tissues and Figure 3F the relationship between the MEbrown module and tumor tissues.

The research team extracted 129 DEGs from ExoRBase datasets and constructed a heatmap to reveal the DEGs (Figure 4A). The Venn diagram (Figure 4B) shows the intersection of three regions, including the DEGs in TCGA-yellow, GEO-brown, and ExoRBase, and the team found only co-differentially expressed MEF2C mRNA (transcription factor). Based on the TCGA database, the expression of MEF2C was significantly lower in CRC tissues (Figures 4C and D) than in normal tissues (Figure 4E).

The MEF2C expression had good predictive effect in evaluating 22 types of immune cells (Figure 5A). Immune cells, such as B cells (Figure 5B), T cell CD8+ (Figure 5C), and activated NK cells (Figure 5D), were associated with MEF2C expression.

Target Genes of MEF2C in CRC

The analysis found 8551 target genes to be associated with MEF2C ($r > 0.5$, $P < .05$). A further search for the potential target genes of MEF2C found 1020 potential target genes of MEF2C in the online version of the database (hTFtarget: http://bioinfo.life.hust.edu.cn/hTFtarget#!/). The intersection of the two regions, one from 8551 target genes and another from 1020 potential target genes, showed that 609 target genes were associated with exosomal MEF2C (Figure6A).

The team determined that 5 was the optimal soft threshold for the adjacency computation. Figures 6B and 6C show that the soft-threshold power value was $\beta = 12$ ($R2 = 0.9$). Figure 6D shows that the dynamic tree cutting approach detected two distinct modules in the RNA co-expression network. As Figure 6E shows, the ME turquoise module was significantly negatively associated with CRC tumors. Heatmaps based on adjacencies showed similar results, as illustrated in the relationships between the ME turquoise module and normal (Figure 6F) and tumor tissues (Figure 6G).

In the GO and KEGG enrichment analyses in the biological-process category, the GO analysis suggested that the DEGs played a forward-mediated role in cytokine production and the regulation of hemopoiesis (Figure 7A). In terms of the cellular component, the secretory granule membrane was the main enriched term. The KEGG terms indicated that significant enrichment, had occurred, which included the C-type, lectin-receptor signaling pathway; parathyroid hormone synthesis, secretion, and action; and an Epstein-Barr viral infection (Figure 7B). Figure 7C lists the top-20 related genes of the PPI networks.

Figures 8A, 8B, and 8C show that high CD36 expression, according to Kaplan-Meier analysis, reflected a longer OS than low CD36 expression did ($P = .044$). In the analysis of the hub genes, the MEF2C was positively related to CD36 (Figure 8D), and the JASPAR analysis revealed a relationship between exosomal MEF2C and CD36 (Figure 8E). Moreover, univariate analysis showed that OS with high CD36 expression was better than OS with low CD36 expression. Overall, these results indicated that CD36 can interact with MEF2C.

Based on TCGA database, the expression of CD36 was significantly lower in CRC

Figure 5. Correlation Between Immune Cells and MEF2C Expression Level. The figures show the correlations between different types of cells and the MEF2C expression level in CRC. Figure 5A shows the correlation between the relative abundance of 22 immune cells and the level; Figure 5B shows the correlation between the relative enrichment score of B cells and the level; Figure 5C shows the correlation between the relative enrichment score of T cell CD8+ and the level; and Figure 5D shows the correlation between the relative enrichment score of activated NK cells and the level.

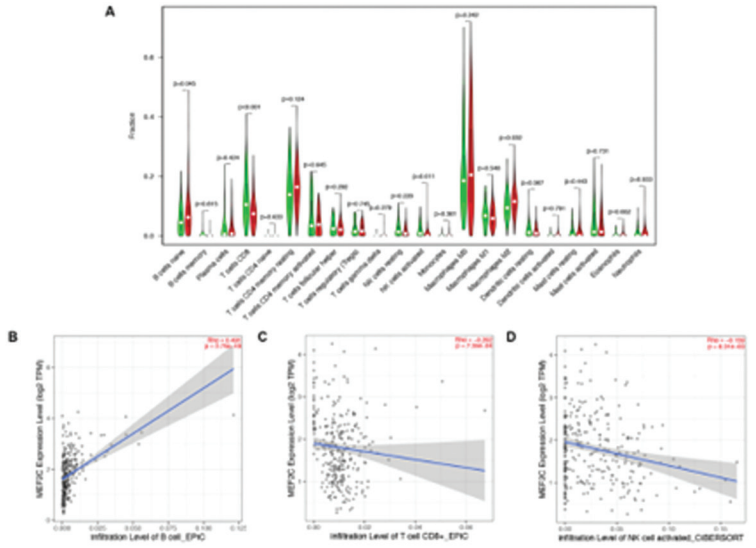

Abbreviations: CRC, colorectal cancer; MEF2C, myocyte enhancer factor 2c–genecards; NK, natural killer.

Figure 6. The Target Genes of MEF2C. Figure 6A shows the Venn diagram for the target genes of MEF2C from the TCGA and online website (hTFtarget:http://bioinfo.life.hust.edu.cn/hTFtarget#!/). and the intersection of the two regions showed that 609 target genes were associated with exosomal MEF2C; Figures 6B and 6C show that the soft-threshold power value was β=12 (R2=0.9); Figure 6D shows that the RNA co-expression network detected two distinct modules using the dynamic tree cutting approach; Figure 6E shows that the MEturquoise module was significantly, negatively associated with CRC tumors; and heat maps based on adjacencies showed similar results, illustrating the relationship between the MEturquoise module and normal (Figure 6F) or tumor (Figure 6G) tissues.

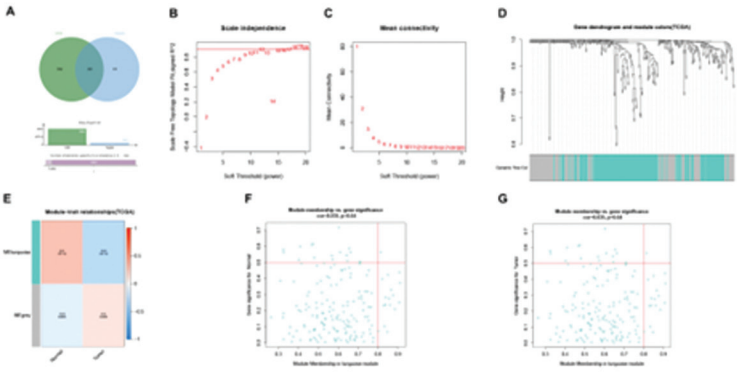

Abbreviations: CRC, colorectal cancer; MEF2C, myocyte enhancer factor 2C–genecards; T cell CD8+, cytotoxic T lymphocytes (CTLs); TCGA, Cancer Genome Atlas database.

Figure 7. GO and KEGG Analysis. Figure 7A shows the GO analysis that was based on the significant genes in the comparison between low- and high-association groups; Figure 7B shows the KEGG pathway analysis of differentially expressed genes, with the rich factor being calculated using the gene count divided by the expected gene count; and Figure 7C shows a PPI network for target genes of MEF2C as visualized by Cytoscape.

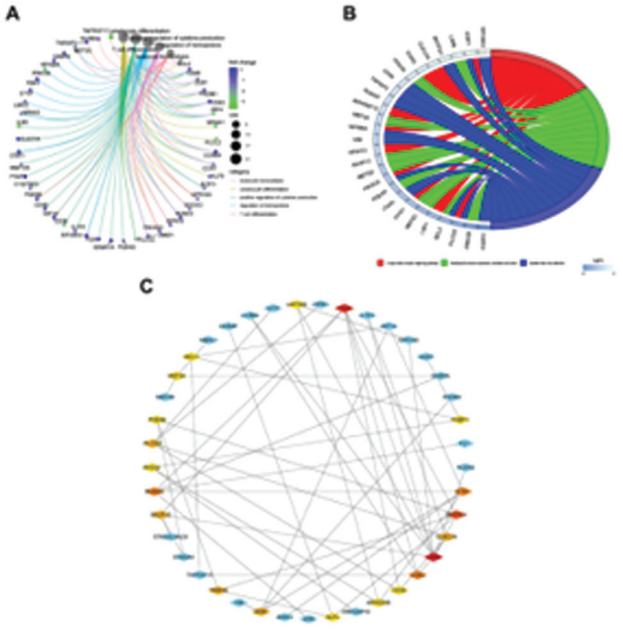

Abbreviations: GO, gene ontology; KEGG, Kyoto Encyclopedia of Genes and Genomes; MEF2C, myocyte enhancer factor 2C–genecards; PPI, protein-protein interaction.

Figure 8. Survival Curve. Figure 8A shows the survival curve of the CD36 in CRC, with a significant correlation being identified between the CD36 and survival outcome in CRC. Figure 8B shows the survival curve of the FNBP1 in CRC, with no significant correlation existing between the FNBP1 and overall survival (OS) in CRC; Figure 8 shows the survival curve of the RUNX3 in CRC, with no significant correlation existing between the RUNX3 and the OS in CRC; Figure 8D shows the correlation analysis between the expression of MEF2C and the expression of CD36, with a significant positive correlation with OS existing; and Figure 8E shows that the JASPAR website predicted the binding regions between MEF2C and CD36.

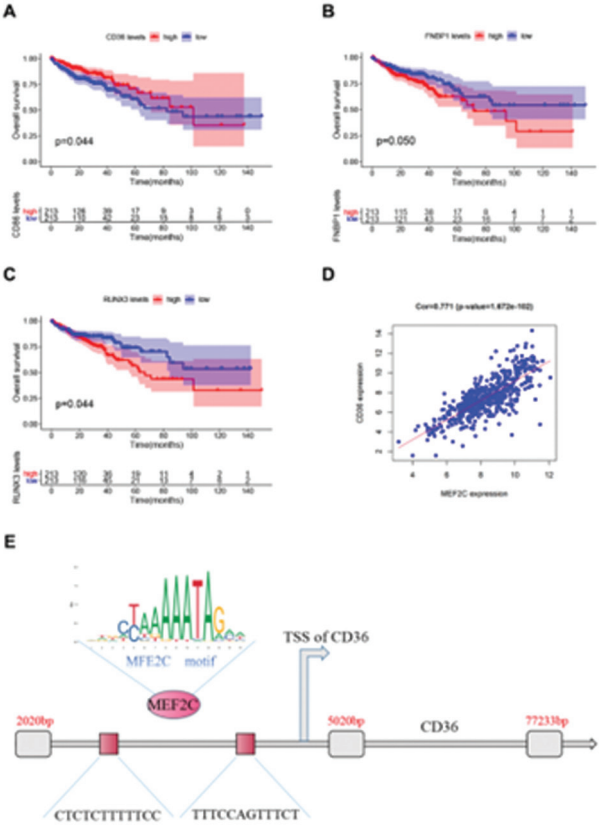

Abbreviations: CD36, cluster of differentiation 36; CRC, colorectal cancer; FNBP1, formin binding protein 1; JASPAR, an open-access database used for transcription factors (TFs) across multiple species in six taxonomic groups; MEF2C, myocyte enhancer factor 2C – genecards; RUNX3, runtrelated transcription factor 3; TSS, transcription start site

tissues (Figure 9A) than in normal tissues (Figure 9B). The prognostic value of CD36 is associated with various subgroups of CRC, including age and T staging (Figure 9C). In the GSEA, the study found many signaling pathways with adjusted $P < .01$ (Figure 9D).

MEF2C and CD36 in CRC

The qPCR analysis of 27 pairs of samples showed that MEF2C and CD36 were downregulated in CRC (Figures 10A and 10B). IHC staining showed low levels of MEF2C and CD36 in CRC (Figures 10C and 10D). These results suggest that both MEF2C and CD36 are low in CRC.

After examining the expression of MEF2C in CRC cell lines, the research team selected SW620 CRC cell line for next study (Figure 11A). Figure 11B shows the particle size experiments, Figure 11C the Western blot assay, and Figure 11D the electron microscopy of the extracted exosomes secreted by SW620. Figure 11E shows the exosome release of SW620 and the SW480 CRC cell line. The results demonstrated that exosomes can effectively deliver MEF2C, suggesting that MEF2C might be a potential biomarker.

Function and Mechanism Analysis of MEF2C in CRC

In the colony-formation assay, MEF2C overexpression inhibited the SW620 CRC cell line's proliferation (Figure 12A) and migration, and invasion (Figure 12B).

The ChIP assay in the SW620 cells showed that the MEF2C was enriched in the 0 to -1600 bp region of the CD36 promoter (Figure 13A). MEF2C enrichment of the CD36 promoter decreased after MEF2C-expression interference (Figure 13B). Meanwhile, the CD36 expression increased after MEF2C overexpression in SW620 (Figure 13C). These results reveal that MEF2C is associated with the CD36 promoter and supports CD36 expression.

Figure 9. The Expression of CD36 in CRC. Figures 9A and 9B show that the expression of CD36, based on the TCGA database, was significantly lower in CRC tissues than in normal tissues; Figures 9C shows the prognostic value of CD36 in the progression-free survival of various subgroups of CRC, including age and T staging; and Figures 9D shows the GSEA results of a reference gene set of a high CD36 expression group.

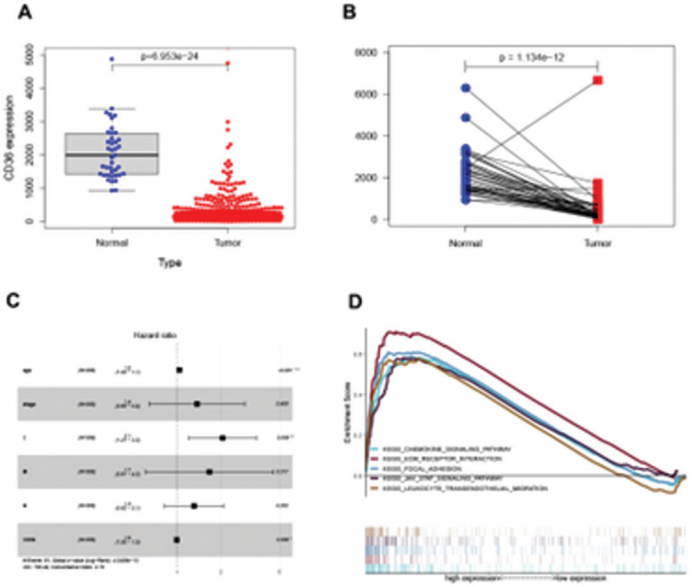

Abbreviations: CD36, cluster of differentiation 36; CRC, colorectal cancer; GSEA, gene set enrichment analysis; KEGG, Kyoto Encyclopedia of Genes and Genomes; TCGA, Cancer Genome Atlas database.

Figure 10. Comparison of the Expression of CD36 and MEF2C in CRC and Normal Tissues. Figures 10A and 10C show the decreased expression of MEF2C, as validated by qRT-PCR and IHC assay; and Figures 10B and 10D show the decreased expression of CD36 as validated by qRT-PCR and IHC assay.

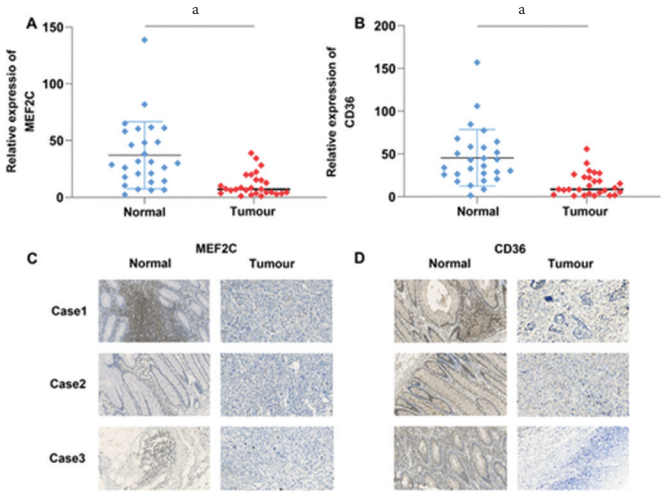

[a]Statistical difference

Abbreviations: CD36, cluster of differentiation 36; CRC, colorectal cancer; IHC, immunohistochemical; MEF2C, MEF2C, myocyte enhancer factor 2C–genecards; qRT-PCR, real-time quantitative reverse transcription-quantitative polymerase chain reaction.

Figure 11. Figure 11A shows that qRT-PCR detected the expression of MEF2C in CRC cell lines, and the research teams selected SW620 for the next study. Figure 11B shows that the NTA identified the presence of exosomes. Figure 11C shows the western blot assay of the protein biomarkers (TSG101 and CD63), and Figure 11D shows the TEM. Figure 11E shows that the western blot validated the presence of MEF2C in the SW480 and SW620 cancer-cell exosomes.

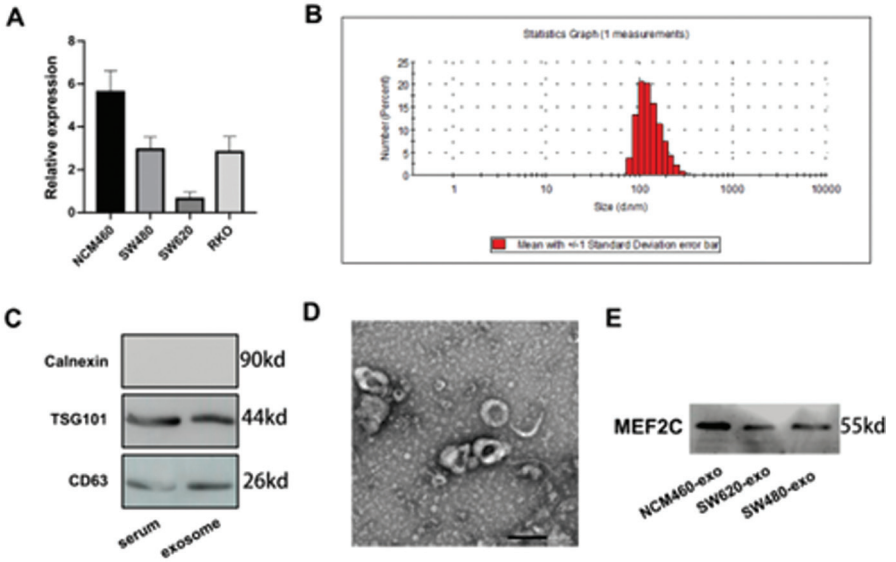

Abbreviations: CRC, colorectal cancer; exo, exosomes; MEF2C, MEF2C, myocyte enhancer factor 2C – genecards; NCM460, normal cell line; NTA, nanoparticle tracking analysis; qRT-PCR, real-time quantitative reverse transcription-quantitative polymerase chain reaction; RKO, CRC cell line; SW480, CRC cell line; SW620, CRC cell line; TEM, transmission electron microscopy; TSG101, tumor susceptibility gene 101 protein

Figure 12. Colony Formation, Cell Migration, and Invasion Assays. The study used these assays to detect the effects of MEF2C on SW620 cell proliferation and invasion. MEF2C overexpression inhibited SW620 cancer-cell proliferation (Figure 12A), migration, and invasion (Figure 12B).

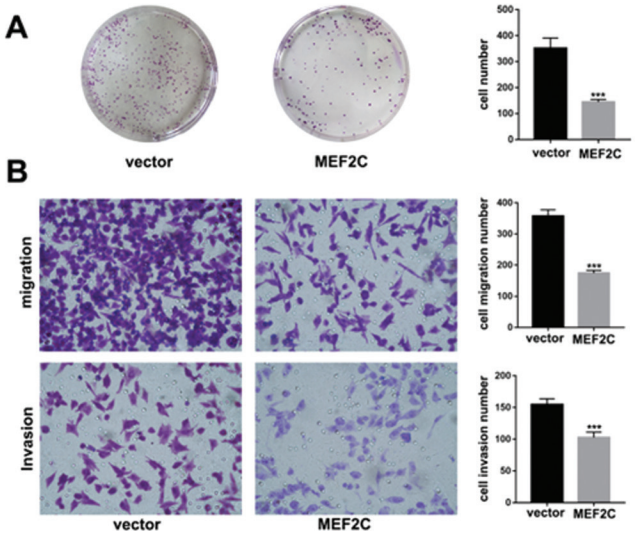

Abbreviations: MEF2C, MEF2C, myocyte enhancer factor 2C – genecards, SW620, CRC cell line

Figure 13. MEF2C Enrichment. Figure 13A shows that the ChIP assays detected the enrichment of MEF2C on the promoter of CD36. A ChIP assay in the SW620 cells showed that MEF2C was enriched in the 0 to -1600 bp region of the CD36 promoter. Figure 13B shows that MEF2C enrichment of the CD36 promoter decreased after MEF2C expression interference in SW620, and Figure 13C shows the expression of CD36 as measured by qRt-PCR after MEF2C overexpression.

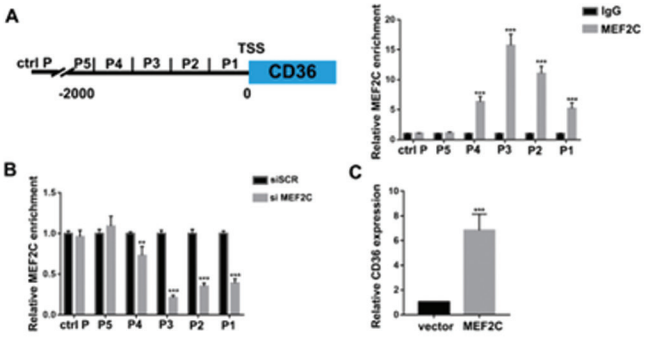

Abbreviations: CD36, cluster of differentiation 36; ChIP, chromatin immunoprecipitation; IgG, immunoglobulin G; MEF2C, MEF2C, myocyte enhancer factor 2C–genecards; qRT-PCR, real-time quantitative reverse transcription-quantitative polymerase chain reaction; siMEF2C (MEF2C knock-down interference sequence); siSCR (MEF2C knockdown negative control sequence); SW620, CRC cell line; TSS, transcriptional start site.

DISCUSSION

The current study found that the yellow module in the TCGA database and the brown module in the GEO database were closely related to CRC progression. The team also found exosome MEF2C by finding the intersection of the yellow module, brown module, and DEGs in the ExoRBase database.

The current research team found that MEF2C couldn't predict the prognosis of CRC, as the ROC curves showed poor predictive value. After performing a correlation analysis ($r > 0.5$, $P < .05$) in the TCGA and the target database, the team associated 609 potential target points with exosomal MEF2C and then assessed them using GO and KEGG, which suggested that MEF2C was associated with the pathway of T-cell differentiation.

Finally, the current study found that CD36 was related to the OS of CRC patients and then investigated the MEF2C and CD36 in CRC samples. The results suggested that MEF2C and CD36 were downregulated in CRC.

Currently no research has investigated MEF2C and its function in CRC. In the current study, the analysis revealed that exosomal MEF2C was lower in CRC tissues, with the MEF2C gene probably being related to the inhibition of CRC. Furthermore, functional experiments suggested that MEF2C overexpression could reduce the progression of SW620 cells, and the current study found positive correlations between MEF2C and immune cells. The current study's examination of mechanisms also found that MEF2C can modulate CD36 transcription, which hadn't been reported previously in CRC.

The current study found that CD36 could improve the five-year OS of CRC patients. Thus, the current research team proposes that the expression of MEF2C can regulate the progression of CRC via CD36. The current research team can reasonably assume that MEF2C is related to immune infiltration, which can offer ways to improve the OS of CRC patients. Therefore, further investigation is needed to probe the immune-related effect of MEF2C in CRC.

The highlights of the article indicate that: (1) exosomes deliver MEF2C, which the current study is the first to report in CRC; and (2) the ChIP assay suggested that MEF2C can suppress CRC progression by regulating CD36 transcription, which also hasn't been reported previously.

However, the current study still had some limitations: (1) although the study yielded meaningful results, the number of samples used was small, and (2) the study didn't analyze the function of MEF2C in vivo. In the subsequent studies, the current research team plans to create a plan for work based on animal experiments.

CONCLUSIONS

MEF2C is a potential biomarker of a favorable prognosis in CRC. MEF2C is related to the progression of CRC. Moreover, the MEF2C-CD36 pathway may reveal the tumor regulation mechanism in CRC. The exosomal MEF2C was the hub gene in exosomes, with CD36 was identified as the potential target. To summarize, exosomal MEF2C may be a promising molecular biomarker for predicting a good prognosis and may have potential as a medical target for CRC.

AVAILABILITY OF DATA AND MATERIALS

The datasets analyzed in this case report are available from the corresponding author on request.

AUTHORS' DISCLOSURE STATEMENT

The research team declares that they have no competing interests. The funders had no role in the study's design, data collection and analysis, decision to publish, or preparation of the manuscript.

ACKNOWLEDGMENTS

Grants from the Beijing Hope Run Special Fund of the Cancer Foundation of China (LC2017A19) supported this work.

REFERENCES

1. Goldstein DA, Ahmad BB, Chen Q, et al. Cost-Effectiveness Analysis of Regorafenib for Metastatic Colorectal Cancer. *J Clin Oncol*. Nov 10 2015;33(32):3727-32. doi:10.1200/JCO.2015.61.9569
2. Bray F, Ferlay J, Soerjomataram I, Siegel RL, Torre LA, Jemal A. Global cancer statistics 2018: GLOBOCAN estimates of incidence and mortality worldwide for 36 cancers in 185 countries. *CA Cancer J Clin*. Nov 2018;68(6):394-424. doi:10.3322/caac.21492
3. Ji D, Zhan T, Li M, et al. Enhancement of Sensitivity to Chemo/Radiation Therapy by Using miR-15b against DCLK1 in Colorectal Cancer. *Stem Cell Reports*. Dec 11 2018;11(6):1506-1522. doi:10.1016/j.stemcr.2018.10.015
4. Liu Y, He X, Pan J, Chen S, Wang L. Prognostic role of Glasgow prognostic score in patients with colorectal cancer: evidence from population studies. *Sci Rep*. Jul 21 2017;7(1):6144. doi:10.1038/s41598-017-06577-2
5. Liang J, Wang WF, Xie S, et al. Expression of beta-transducin repeat-containing E3 ubiquitin protein ligase in human glioma and its correlation with prognosis. *Oncol Lett*. Jun 2015;9(6):2651-2656. doi:10.3892/ol.2015.3113
6. Linnekamp JF, Hooff SRV, Prasetyanti PR, et al. Consensus molecular subtypes of colorectal cancer are recapitulated in in vitro and in vivo models. *Cell Death Differ*. Mar 2018;25(3):616-633. doi:10.1038/s41418-017-0011-5
7. Li L, Li C, Wang S, et al. Exosomes Derived from Hypoxic Oral Squamous Cell Carcinoma Cells Deliver miR-21 to Normoxic Cells to Elicit a Prometastatic Phenotype. *Cancer Res*. Apr 1 2016;76(7):1770-80. doi:10.1158/0008-5472.CAN-15-1625
8. Kahlert C, Kalluri R. Exosomes in tumor microenvironment influence cancer progression and metastasis. *J Mol Med (Berl)*. Apr 2013;91(4):431-7. doi:10.1007/s00109-013-1020-6
9. Kim MS, Haney MJ, Zhao Y, et al. Engineering macrophage-derived exosomes for targeted paclitaxel delivery to pulmonary metastases: in vitro and in vivo evaluations. *Nanomedicine*. Jan 2018;14(1):195-204. doi:10.1016/j.nano.2017.09.011
10. Camussi G, Deregibus MC, Bruno S, Cantaluppi V, Biancone L. Exosomes/microvesicles as a mechanism of cell-to-cell communication. *Kidney Int*. Nov 2010;78(9):838-48. doi:10.1038/ki.2010.278
11. Chen X, Liu J, Zhang Q, et al. Exosome-mediated transfer of miR-93-5p from cancer-associated fibroblasts confer radioresistance in colorectal cancer cells by downregulating FOXA1 and upregulating TGFB3. *J Exp Clin Cancer Res*. Apr 15 2020;39(1):65. doi:10.1186/s13046-019-1507-2
12. Yin H, Hu J, Ye Z, Chen S, Chen Y. Serum long noncoding RNA NNTAS1 protected by exosome is a potential biomarker and functions as an oncogene via the miR496/RAP2C axis in colorectal cancer. *Mol Med Rep*. Aug 2021;24(2)doi:10.3892/mmr.2021.12224
13. Barrett T, Wilhite SE, Ledoux P, et al. NCBI GEO: archive for functional genomics data sets--update. *Nucleic Acids Res*. Jan 2013;41(Database issue):D991-5. doi:10.1093/nar/gks1193
14. Li X, Wang X, Zhao J, Wang J, Wu J. PRMT5 promotes colorectal cancer growth by interaction with MCM7. *J Cell Mol Med*. Apr 2021;25(7):3537-3547. doi:10.1111/jcmm.16436
15. Chen J, He Q, Wu P, et al. ZMYND8 expression combined with pN and pM classification as a novel prognostic prediction model for colorectal cancer: Based on TCGA and GEO database analysis. *Cancer Biomark*. 2020;28(2):201-211. doi:10.3233/CBM-191261
16. Yang Z, An Y, Wang N, Dong X, Kang H. LINC02595 promotes tumor progression in colorectal cancer by inhibiting miR-203b-3p activity and facilitating BCL2L1 expression. *J Cell Physiol*. Oct 2020;235(10):7449-7464. doi:10.1002/jcp.29650
17. Li S, Li Y, Chen B, et al. exoRBase: a database of circRNA, lncRNA and mRNA in human blood exosomes. *Nucleic Acids Res*. Jan 4 2018;46(D1):D106-D112. doi:10.1093/nar/gkx891
18. Papavassiliou KA, Papavassiliou AG. Transcription Factor Drug Targets. *J Cell Biochem*. Dec 2016;117(12):2693-2696. doi:10.1002/jcb.25605
19. Yan TT, Fu XL, Li J, et al. Downregulation of RPL15 may predict poor survival and associate with tumor progression in pancreatic ductal adenocarcinoma. *Oncotarget*. Nov 10 2015;6(35):37028-42. doi:10.18632/oncotarget.5939
20. Potthoff MJ, Olson EN. MEF2: a central regulator of diverse developmental programs. *Development*. Dec 2007;134(23):4131-40. doi:10.1242/dev.008367
21. Latchman DS. Transcription factors: an overview. *Int J Biochem Cell Biol*. Dec 1997;29(12):1305-12. doi:10.1016/s1357-2725(97)00085-x
22. Kim J, Bae JS. Tumor-Associated Macrophages and Neutrophils in Tumor Microenvironment. *Mediators Inflamm*. 2016;2016:6058147. doi:10.1155/2016/6058147
23. Tosolini M, Kirilovsky A, Mlecnik B, et al. Clinical impact of different classes of infiltrating T cytotoxic and helper cells (Th1, th2, treg, th17) in patients with colorectal cancer. *Cancer Res*. Feb 15 2011;71(4):1263-71. doi:10.1158/0008-5472.CAN-10-2907
24. Galon J, Costes A, Sanchez-Cabo F, et al. Type, density, and location of immune cells within human colorectal tumors predict clinical outcome. *Science*. Sep 29 2006;313(5795):1960-4. doi:10.1126/science.1129139
25. Pages F, Kirilovsky A, Mlecnik B, et al. In situ cytotoxic and memory T cells predict outcome in patients with early-stage colorectal cancer. *J Clin Oncol*. Dec 10 2009;27(35):5944-51. doi:10.1200/JCO.2008.19.6147
26. Cui F, Qu D, Sun R, Zhang M, Nan K. NK cell-produced IFN-gamma regulates cell growth and apoptosis of colorectal cancer by regulating IL-15. *Exp Ther Med*. Feb 2020;19(2):1400-1406. doi:10.3892/etm.2019.8343
27. Ma C, Jin RM, Chen KJ, et al. Low expression of B-Cell-Associated protein 31 is associated with unfavorable prognosis in human colorectal cancer. *Pathol Res Pract*. May 2018;214(5):661-666. doi:10.1016/j.prp.2018.03.023

28. Zhang H, Liu W, Wang Z, et al. MEF2C promotes gefitinib resistance in hepatic cancer cells through regulating MIG6 transcription. *Tumori*. Jun 2018;104(3):221-231. doi:10.1177/0300891618765555
29. Luo T, Zhao J, Lu Z, et al. Characterization of long non-coding RNAs and MEF2C-AS1 identified as a novel biomarker in diffuse gastric cancer. *Transl Oncol*. Oct 2018;11(5):1080-1089. doi:10.1016/j.tranon.2018.06.007
30. Bishop JA, Weinreb I, Swanson D, et al. Microsecretory Adenocarcinoma: A Novel Salivary Gland Tumor Characterized by a Recurrent MEF2C-SS18 Fusion. *Am J Surg Pathol*. Aug 2019;43(8):1023-1032. doi:10.1097/PAS.0000000000001273
31. Tarumoto Y, Lu B, Somerville TDD, et al. LKB1, Salt-Inducible Kinases, and MEF2C Are Linked Dependencies in Acute Myeloid Leukemia. *Mol Cell*. Mar 15 2018;69(6):1017-1027 e6. doi:10.1016/j.molcel.2018.02.011
32. Agatheeswaran S, Chakraborty S. MEF2C and CEBPA: Possible co-regulators in chronic myeloid leukemia disease progression. *Int J Biochem Cell Biol*. Aug 2016;77(Pt A):165-170. doi:10.1016/j.biocel.2016.06.007
33. Singh J, Kumar R, Verma D, et al. MEF2C expression, but not absence of bi-allelic deletion of TCR gamma chains (ABD), is a predictor of patient outcome in Indian T-acute lymphoblastic leukemia. *Am J Blood Res*. 2020;10(5):294-304.
34. Drury J, Rychahou PG, Kelson CO, et al. Upregulation of CD36, a Fatty Acid Translocase, Promotes Colorectal Cancer Metastasis by Increasing MMP28 and Decreasing E-Cadherin Expression. *Cancers (Basel)*. Jan 5 2022;14(1)doi:10.3390/cancers14010252
35. Silverstein RL, Febbraio M. CD36 and atherosclerosis. *Curr Opin Lipidol*. Oct 2000;11(5):483-91. doi:10.1097/00041433-200010000-00006
36. Febbraio M, Hajjar DP, Silverstein RL. CD36: a class B scavenger receptor involved in angiogenesis, atherosclerosis, inflammation, and lipid metabolism. *J Clin Invest*. Sep 2001;108(6):785-91. doi:10.1172/JCI14006
37. Chen YJ, Liao WX, Huang SZ, et al. Prognostic and immunological role of CD36: A pan-cancer analysis. *J Cancer*. 2021;12(16):4762-4773. doi:10.7150/jca.50502
38. Zhang X, Yao J, Shi H, Gao B, Zhang L. LncRNA TINCR/microRNA-107/CD36 regulates cell proliferation and apoptosis in colorectal cancer via PPAR signaling pathway based on bioinformatics analysis. *Biol Chem*. Apr 24 2019;400(5):663-675. doi:10.1515/hsz-2018-0236
39. Tsuchida T, Kijima H, Tokunaga T, et al. Expression of the thrombospondin 1 receptor CD36 is correlated with decreased stromal vascularisation in colon cancer. *Int J Oncol*. Jan 1999;14(1):47-51.
40. Love MI, Huber W, Anders S. Moderated estimation of fold change and dispersion for RNA-seq data with DESeq2. *Genome Biol*. 2014;15(12):550. doi:10.1186/s13059-014-0550-8
41. Drury J, Rychahou PG, He D, et al. Inhibition of Fatty Acid Synthase Upregulates Expression of CD36 to Sustain Proliferation of Colorectal Cancer Cells. *Front Oncol*. 2020;10:1185. doi:10.3389/fonc.2020.01185
42. Heath AP, Ferretti V, Agrawal S, et al. The NCI Genomic Data Commons. *Nat Genet*. Mar 2021;53(3):257-262. doi:10.1038/s41588-021-00791-5
43. Zhuang H, Huang S, Zhou Z, et al. A four prognosis-associated lncRNAs (PALnc) based risk score system reflects immune cell infiltration and predicts patient survival in pancreatic cancer. *Cancer Cell Int*. 2020;20:493. doi:10.1186/s12935-020-01588-y
44. Kanehisa M, Goto S. KEGG: kyoto encyclopedia of genes and genomes. *Nucleic Acids Res*. Jan 1 2000;28(1):27-30. doi:10.1093/nar/28.1.27
45. Kramer A, Green J, Pollard J, Jr., Tugendreich S. Causal analysis approaches in Ingenuity Pathway Analysis. *Bioinformatics*. Feb 15 2014;30(4):523-30. doi:10.1093/bioinformatics/btt703
46. Liu Q, Wang C, Jiao X, et al. Hi-TOM: a platform for high-throughput tracking of mutations induced by CRISPR/Cas systems. *Sci China Life Sci*. Jan 2019;62(1):1-7. doi:10.1007/s11427-018-9402-9
47. Khan A, Mathelier A. JASPAR RESTful API: accessing JASPAR data from any programming language. *Bioinformatics*. May 1 2018;34(9):1612-1614. doi:10.1093/bioinformatics/btx804
48. Cooley Coleman JA, Sarasua SM, Boccuto L, Moore HW, Skinner SA, DeLuca JM. Comprehensive investigation of the phenotype of MEF2C-related disorders in human patients: A systematic review. *Am J Med Genet A*. Dec 2021;185(12):3884-3894. doi:10.1002/ajmg.a.62412